Available online at www.sciencedirect.com
ScienceDirect
Mendeleev Commun., 2015, **25**, 358–360
Mendeleev Communications

Mesoporic material from microcrystalline cellulose with gold nanoparticles: a new approach to metal-carrying polysaccharides

Alexander Yu. Vasil'kov,*[a] Margarita S. Rubina,[a] Albina A. Gallyamova,[b] Alexander V. Naumkin,[a] Michael I. Buzin[a] and Galina P. Murav'eva[b]

[a] *A. N. Nesmeyanov Institute of Organoelement Compounds, Russian Academy of Sciences, 119991 Moscow, Russian Federation. Fax: +7 499 135 9380; e-mail: alexandervasilkov@yandex.ru*
[b] *Department of Chemistry, M. V. Lomonosov Moscow State University, 119991 Moscow, Russian Federation*

DOI: 10.1016/j.mencom.2015.09.014

The mesoporic hybrid material was prepared from microcrystalline cellulose modified with gold nanoparticles by metal-vapor synthesis.

Porous nanocomposites based on polysaccharides are widely used in cosmetic and medical fields and for the production of carbon materials, catalytic supports *etc*.[1] Cellulose is of special interest because the modification of this natural polymer with metal nanoparticles (NPs) gives special magnetic, catalytic and antibacterial properties to the material.[1,2] For example, cellulose modified with Ag NPs exhibits high antibacterial properties.[3]

Methods for modifying cellulose with metal NPs are based on metal recovery from precursors, such as metal salts, metal complexes and other metal compounds introduced into the polymer.[4] As a rule, polymers modified with metals require an additional cleaning procedures to remove the decomposition products of the complex, the reducing agent, surfactants or other compounds used in the synthesis of metal NPs. Metal-vapor synthesis (MVS) is free of these disadvantages and affords mono- and bimetallic NPs[5] and materials based on them.[6] Metal NPs synthesized by MVS are in the non-oxidized form, the formation of materials occurs at temperatures up to 300 K, which allow the polymer to avoid degradation.

The formation of porous polymer structure promotes effective stabilization and more uniform distribution of NPs in polymer surface layers. For instance, porous cellulose can be produced by direct dissolving cellulose in an aqueous alkali followed by precipitation and freeze drying.[7]

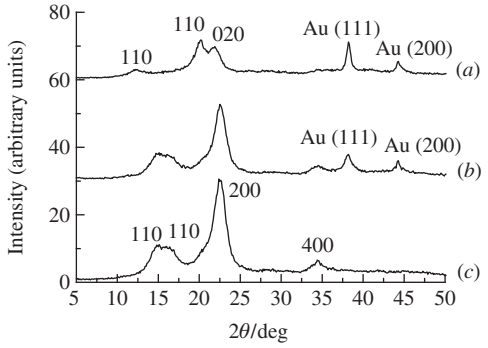

Figure 1 XRD patterns: (*a*) Au/porous MCC, (*b*) Au/powder MCC and (*c*) MCC.

The XRD patterns of MCC [Figure 1(*a*)] and Au/powder MCC† [Figure 1(*b*)] show peaks characteristic of native cellulose[10]

† Metal-carrying polymer composite was prepared by the impregnation of microcrystalline cellulose (MCC) (Avicel PH-101; degree of polymerization, 180; Sigma Aldrich) with an Au organosol in Pr^{i}OH which was distilled from molecular sieves (4 Å) and degassed in a vacuum by freezing–thawing cycles. The organosol was prepared by MVS according to a procedure described elsewhere.[8] Gold (99.99%) was evaporated by resistively heating a tungsten rod (d = 1.5 mm) at a residual pressure of 10^{-2} Pa. In a typical experiment, the metal and Pr^{i}OH vapor were condensed on liquid nitrogen-cooled walls of a 5-l reactor. Next, the deposit was melted, and the resulting metal organosol was infiltrated into MCC in an evacuated Schlenk vessel. The excess organosol was removed, and the support was dried in a vacuum of 1 Pa at 90 °C for 1 h. At the final stage, the powder of MCC containing gold nanoparticles was obtained (Au/powder MCC). All manipulations were performed in a pure Ar atmosphere.

The sol-gel technology[9] combined with freeze-drying was used for preparing cellulose with porous structure. Firstly, Au/powder MCC was mixed with water and kept for 2 h at 5 °C to allow fiber swelling. Then, the blend was cooled at –6 °C, and aqueous alkali precooled at –6 °C was added. For preparing a 100-ml solution, 5 g of MCC in 60 ml of water and 7.6 g of NaOH in 40 ml of water were taken. Mixing was performed at –6 °C for 2 h with a stirring rate of 1000 rpm. After 2 h, the solution was poured into cylindrical molds, in which gelation occurred at 60 °C for 2 h. Then, the cylindrical blocks of MCC with gold nanoparticles were washed with water to remove NaOH. The regenerated block was cooled to –12 °C in a refrigerator and subjected to freeze-drying in a vacuum at 1 Pa and at room temperature. Finally, porous structure of MCC with gold nanoparticles (Au/porous MCC) was obtained.

The Au concentration in the sample was determined on a VRA 30 X-ray fluorescent analyzer (Germany) using the Au Lα line.

The X-ray diffractometry (XRD) of the samples was performed in reflection mode (Stoe Stad P, Germany) with CuKα radiation (λ = = 0.15406 nm) in the range of 2θ = 5–40°. The crystallite sizes were estimated with full-width half-maximum of respective diffraction peaks.

The XPS measurements were performed with Quantera SXM (Physical Electronics, USA) using an Al Kα X-ray source (1486.6 eV). The spectra were measured at room temperature and the pressure in the sample analysis chamber was ~5×10^{-8} Pa. The binding energy scale was calibrated against the peaks of Au $4f_{7/2}$ (84.0 eV), Ag $3d_{5/2}$ (368.3 eV) and Cu $2p_{3/2}$ (932.7 eV).

Thermogravimetric analysis (TGA) and dynamic thermogravimetric analysis (DTA) were carried out on a DerivatographC (MOM, Hungary) at a scan rate of 10 K min^{-1} from room temperature to 800 °C in air and argon atmospheres, respectively.

Nitrogen physisorption measurements at 77 K were performed on a Gemini VII 2390 (V1, 02 t) instrument (Micrometrics, USA). Before the analysis the samples were degassed at 300 °C for 12 h in a vacuum to remove the adsorbed species. The Brunauer–Emmett–Teller (BET) and Barrett–Jyner–Halenda (BJH) analyses were done by the standard software. Specific surface areas were calculated by the BET model for a relative vapor pressure of 0.2. The total pore volume and pore radius distribution were calculated by the BJH model for a relative vapor pressure of 0.95.

(cellulose I). These peaks are located at 15°, 16°, 12.5° and 34.8°, which are assigned to (1$\bar{1}$0), (110), (200) and (400) crystallographic planes, respectively. Additional peaks at 38° and 44° correspond to the (111) and (200) crystallographic plane reflections of gold, respectively. Comparison of the two spectra [Figure 1(*a*),(*b*)] shows that the modification of cellulose with gold NPs does not alter its structure and crystallinity. However, the aqueous alkali impact on Au/powder MCC leads to amorphisation and changes in its crystal structure. The XRD pattern of Au/porous MCC [Figure 1(*c*)] exhibits peaks at 12°, 20° and 21.7°, which are assigned to (1$\bar{1}$0), (110) and (020) crystallographic planes of cellulose II polymorph, respectively.[11] This change in cellulose crystalline structure is irreversible and normally accompanied by a decrease in the crystallinity.[11] XRD shows a decrease in the crystallinity index (Cr.I.) for Au/porous MCC (Cr.I. = 0.66) in comparison with that of MCC (Cr.I. = 0.83). According to XRD data, the average particle size may be assessed as 10.2 (Au/powder MCC) or 16.6 nm (Au/porous MCC). Thus, the treatment of Au/powder MCC with an alkaline solution and the subsequent freeze-drying result in the aggregation of NPs in the polymer matrix.

The surface composition and chemical state of gold in Au/porous MCC were characterized by XPS. The Au 4*f* spectrum (Figure 2) is fitted with two Gaussian profiles at binding energies of 84.0 and 87.7 eV with widths of 1.0 and 0.9 eV, respectively, and a branching ratio of 1.33. The peaks are assigned to Au $4f_{7/2}$ and Au $4f_{5/2}$ levels and related to Au^0 state. The relative concentration of gold was 0.30 wt%. This value is close to the elemental analysis data (0.34 wt%). The proximity of the gold contents may be indicative of the homogeneity of the composite material.

The thermal stability of the nanocomposites was measured with TGA and DSC. TGA curves in air and argon for MCC and Au/porous MCC demonstrate a slight step of weight loss (~3%) at 100–120 °C, corresponding to the loss of hydrated and coordinated water molecules, which come from the environment [Figure 3(*a*)]. The decomposition of the samples in air occurs in two stages, the first of which terminates at 360 °C [Figure 3(*a*)]. At this stage, the temperatures of the decomposition rate maximum [position of the minimum of the corresponding peaks in the DTG curves in Figure 3(*b*)] for MCC and Au/porous MCC are similar, while the decomposition onset temperature is higher for the MCC. The weight loss at this stage of MCC degradation is significantly higher (67 wt%) than that observed for Au/MCC porous (55 wt%). The end of the second stage for Au/porous MCC is 630 °C, which is 100 °C higher than that of MCC. DTA curves exhibit two exothermic peaks at positions on the temperature scale which are consistent with the TGA data and correspond to thermo-oxidative cellulose transformations [Figure 3(*c*)]. Decomposition of MCC and Au/porous MCC in an argon atmosphere occurs in a single step, which coincides in temperature with the first stage of decomposition observed in air. The significant carbonation of the solid residue proceeds during the Au/porous MCC decomposition in an inert atmosphere, the amount of which is 30 wt% and twice greater than that of MCC. A similar effect was observed for gold–cellulose aerogel subjected to carbonization.[12] This can indicate that gold nanoparticles have specific interference with cellulose decomposition, which might be attributed to the catalytic effect of gold NPs altering cellulose decomposition.[12]

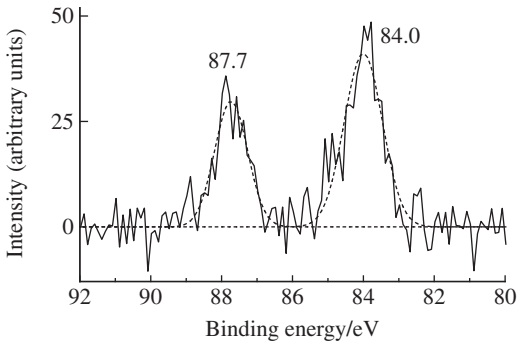

Figure 2 Au 4*f* photoelectron spectrum of Au/porous MCC.

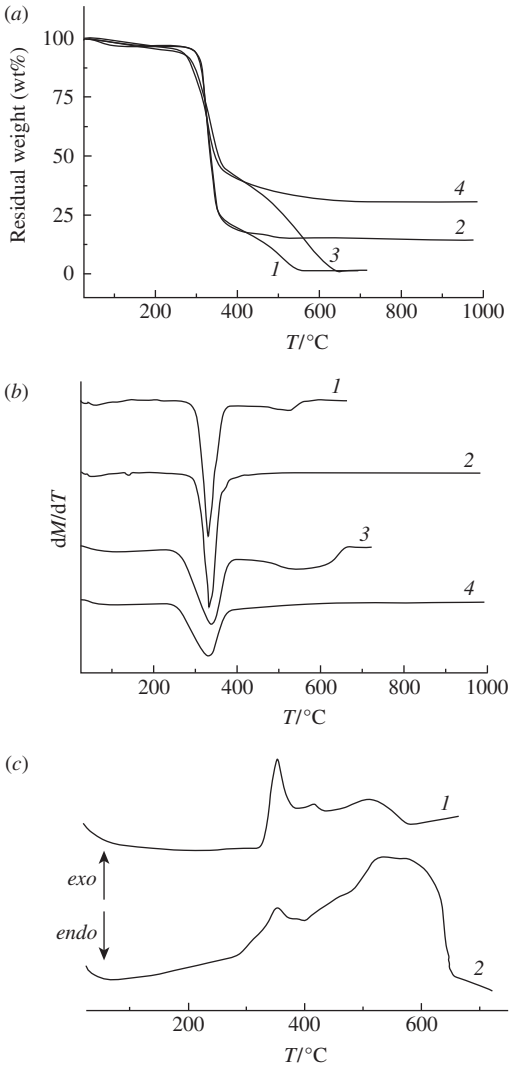

Figure 3 (*a*), (*b*) TGA and (*c*) DTA curves for (*1*, *3*) MCC and (*2*, *4*) Au-MCC/porous in (*1*, *2*) air and (*3*, *4*) argon at a scan rate of 10 K min^{-1}.

Nitrogen porosimetry analysis revealed the mesoporous nature of Au/porous MCC (*i.e.* a Type IV isotherm). The BET surface area was 40 m^2 g^{-1}. Pore size distribution of Au/porous MCC is shown in Figure 4.

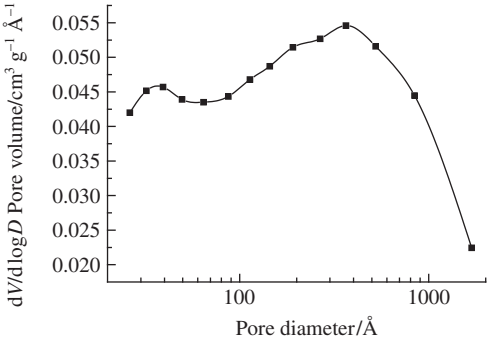

Figure 4 Qualitative pore size distribution in Au/porous MCC obtained by BJH analysis.

In conclusion, a new method for preparing metal-bearing mesoporic polysaccharides has been reported. The mesoporic cellulose with gold nanoparticles was prepared by a combination of metal-vapor synthesis, sol-gel technology and freeze-drying. The average size of gold nanoparticles in the metal-bearing polymer was 16.6 nm. According to XPS data, gold atoms occured in a metallic state; the binding energies of the Au $4f_{7/2}$ and Au $4f_{5/2}$ peaks were 84.0 and 87.7 eV, respectively.

This work was supported by the Russian Foundation for Basic Research (grant nos. 14-03-01074 and 15-53-61030) and the Russian Academy of Sciences (DCMS Programme nos. 4 and 6).

References

1 (*a*) T. Mehling, I. Smirnova, U. Guenther and R. H. H. Neubert, *J. Non-Cryst. Solids*, 2009, **355**, 2472; (*b*) V. Budarin, J. H. Clark, J. J. E. Hardy, R. Luque, K. Milkowski, S. J. Tavener and A. J. Wilson, *Angew. Chem. Int. Ed*., 2006, **45**, 3782; (*c*) E. Guilminot, R. Gavillon, M. Chatenet, S. Berthon-Fabryc, A. Rigacci and T. Budtova, *J. Power Sources*, 2008, **185**, 717.

2 (*a*) C. A. García-González, E. Carenza, M. Zeng, I. Smirnova and A. Roig, *RSC Adv.*, 2012, **2**, 9816; (*b*) W. K. Son, J. H. Youk and W. H. Park, *Carbohydr. Polym.*, 2006, **65**, 430.

3 S.-M. Li, N. Jia, J.-F. Zhu, M.-G. Ma, F. Xu, B. Wang and R.-C. Sun, *Carbohydr. Polym*., 2011, **83**, 422.

4 (*a*) G. Yang, J. Xie, F. Hong, Z. Cao and X. Yang, *Carbohydr. Polym.*, 2012, **87**, 839; (*b*) S.-M. Li, N. Jia, M.-G. Ma, Z. Zhang, Q.-H. Liu and R.-C. Sun, *Carbohydr. Polym.*, 2011, **86**, 441; (*c*) L. C. de Santa Maria, A. L. C. Santos, P. C. Oliveira, H. S. Barud, Y. Messaddeq and S. J. L. Ribeiro, *Mater. Lett*., 2009, **63**, 797.

5 (*a*) A. B. Smetana, K. J. Klabunde and C. M. Sorensen, *J. Colloid Interface Sci*., 2005, **284**, 521; (*b*) A. N. Karavanov, V. M. Gryaznov, V. I. Lebedeva, I. A. Litvinov, A. Yu. Vasil'kov and A. Yu. Olenin, *Catal. Today*, 1995, **25**, 447; (*c*) V. G. Nenajdenko, A. Yu. Vasil'kov, A. A. Goldberg, V. M. Muzalevskiy, A. V. Naumkin, V. L. Podshibikhin, A. V. Shastin and E. S. Balenkova, *Mendeleev Commun.*, 2010, **20**, 200.

6 (*a*) A. Yu. Vasil'kov, S. A. Nikolaev, V. V. Smirnov, A. V. Naumkin, I. O. Volkov and V. L. Podshibikhin, *Mendeleev Commun*., 2007, **17**, 268; (*b*) A. Yu. Vasil'kov, B. A. Zachernyuk, Z. N. Karpikov, I. O. Volkov, Y. V. Zubavichus, A. A. Veligzhanin, A. A. Chernyshov, M. I. Buzin and L. N. Nikitin, *Russ. J. Appl. Chem*., 2007, **80**, 2136 (*Zh. Prikl. Khim.*, 2007, **80**, 2058); (*c*) G. Cardenas, J. Diaz V., M. F. Melendrez, C. Cruzat C. and A. Garsía Cancino, *Polym. Bull*., 2009, **62**, 511.

7 J. Cai, S. Kimura, M. Wada, S. Kuga and L. Zhang, *ChemSusChem*, 2008, **1**, 149.

8 A. Yu. Vasil'kov, A. V. Naumkin, I. O. Volkov, V. L. Podshibikhin, G. V. Lisichkin and A. R. Khokhlov, *Surf. Interface Anal*., 2010, **42**, 559.

9 (*a*) R. Gavillon and T. Budtova, *Biomacromolecules*, 2008, **9**, 269; (*b*) R. Sescousse, R. Gavillon and T. Budtova, *Carbohydr. Polym*., 2011, **83**, 1766.

10 S. Y. Oh, D. I. Yoo, Y. Shin, H. C. Kim, H. Y. Kim, Y. S. Chung, W. H. Park and J. H. Youk, *Carbohydr. Res*., 2005, **340**, 2376.

11 P. K. Gupta, V. Uniyal and S. Naithani, *Carbohydr. Polym*., 2013, **94**, 843.

12 J. Cai, S. Kimura, M. Wada and S. Kuga, *Biomacromolecules*, 2009, **10**, 87.

Received: 13th March 2015; Com. 15/4584